Ternary Phase Diagrams of Poly(styrene-*co*-methyl methacrylate), Poly(methyl methacrylate), and Polystyrene: Monomer Sequence Distribution Effect and Encapsulation

Karen I. Winey* and Maria Luisa Berba[†]

Laboratory for Research on the Structure of Matter, Department of Materials Science and Engineering, University of Pennsylvania, Philadelphia, Pennsylvania 19104-6272

Mary E. Galvin

AT&T Bell Laboratories, Murray Hill, New Jersey 07974

Received September 22, 1995; Revised Manuscript Received January 22, 1996[⊗]

ABSTRACT: The phase behavior in ternary blends of polystyrene (PS), poly(methyl methacrylate) (PMMA), and poly(styrene-*co*-methyl methacrylate) has been determined as a function of sequence distribution at 150 °C. Two copolymers were investigated which have comparable compositions (48−50 mol % methyl methacrylate monomer units) but distinct sequence distributions, namely strictly alternating and random. The phase behavior was determined via transmission electron microscopy, which found the number of phases, the relative amounts of the phases, and the spatial arrangement of the phases. Equilibrium blend compositions were calculated from the experimental results using mass balance equations. These equilibrium compositions were used to construct isothermal ternary phase diagrams which exhibited three pairwise immiscible binary systems and a three-phase region. From these ternary phase diagrams, we show that the compositionally symmetric copolymers are more miscible in PMMA than PS and that this asymmetry in miscibility is more pronounced with the alternating sequence. This sequence distribution effect is discussed in terms of specific interactions between the methyl methacrylate monomer units. With either alternating or random copolymers, the three-phase blends exhibit encapsulation when the copolymer-rich phase is less than 25 vol % of the blend; otherwise the copolymer-rich phase forms a continuous matrix. The equilibrium compositions of binary blends containing poly(methyl methacrylate) and a copolymer were also investigated as a function of molecular weight.

Introduction

The microstructure of polymers, including tacticity, branching, and monomer sequence distribution, is being controlled to ever increasing extents and, subsequently, polymer scientists are continuing to uncover the influence of these structural attributes on polymer properties. The sequence distribution describes the order of the monomer units along a copolymer chain. Improvements in characterization techniques, particularly nuclear magnetic resonance, permit the determination of the sequence distribution by distinguishing the various triads and pentads within copolymers. Certainly the importance of large differences in sequence distribution is well-established; for example, a block copolymer microphase separates into periodic microdomains while at the same temperature a random copolymer of the same monomer units, copolymer composition, and molecular weight is homogeneous. Smaller differences in sequence distribution are now being investigated with regard to their discoloration properties[1] and blend miscibility.[2−8] The majority of these blend miscibility studies on the effect of sequence distribution have involved chlorinated polyethylene, poly(vinyl chloride), or chlorinated poly(vinyl chloride).[2−5,7] These copolymers, which contain primarily CH_2 and CHCl units in various sequences and to a lesser extent CCl_2 due to the chlorination process, possess a large halogen atom. Reports of sequence distribution in non-halogen-containing polymers have been limited to the study of substantial differences in the sequence distribution[8] or limited by the experimental techniques used.[9,6]

Even before the experimental evidence for the importance of sequence distribution effects began to accumulate, theories and simulations were being developed to treat this issue. Balazs et al.[10−12] and subsequently Cantow et al.[13] have introduced triad−triad interaction parameters, rather than monomer−monomer interaction parameters, to describe the blend thermodynamics. These triad interaction parameters are used to compute an interaction parameter for the blend according to the relative amounts of the various triads, which defines the sequence distribution. Specifically, Balazs et al. calculated ternary phase diagrams for an AB copolymer with A and B homopolymers as a function of the sequence distribution in the copolymers.[12] It is this work that was the initial inspiration for our studies initiated by Galvin.[9] Previous researchers have applied the Balazs or Cantow theories to determine triad interaction parameters based on miscibility experiments on binary blends.[2,5] However, because triad−triad interaction parameters are difficult to measure independently,[14] rigorous evaluations of these theories are still absent. More recently, a number of modifications have been applied to mean field theory to incorporate the composition[15] and microstructure[16,17] complexities of random copolymer systems and multiblock copolymer/homopolymer blends.

Phase diagrams provide two types of information: the equilibrium compositions of the coexisting phases and the relative amounts of these phases for a given blend composition. Binary polymer blends of various compositions and corresponding to specific temperatures are typically probed via differential scanning calorimetry and/or light scattering to determine the number of phases (one or two) present. These results are typically plotted on a binary phase diagram (temperature vs

[†] Current address: Johnson & Johnson Philippines, Inc., Manila.

[⊗] Abstract published in *Advance ACS Abstracts,* March 1, 1996.

0024-9297/96/2229-2868$12.00/0

blend composition) and a curve is drawn separating the miscible and immiscible blends. The resolution of such phase diagrams is determined by the proximity between the studied blends and the equilibrium composition, while the accuracy of these diagrams depends on the ability of DSC and cloud point measurements to detect the number of phases present. Ternary mixtures have been studied in a similar manner though the distinction between two and three phases has not typically been made.[18−23]

Industrial applications require that polymer blends become more complex both in the intricacies of the individual components and in the number of components. Increasing the number of polymer components is a complication which obviously provides enhanced design flexibility for the control of multiple properties. Whereas scientific studies of ternary polymer blends were virtually unknown a decade ago, there is a growing body of experimental results in this field primarily addressing systems with either two[18−22,24,25] or three[23,25−27] pairs of miscible polymers. When all three binary pairs (A−B, A−C, B−C) are miscible, isothermal ternary phase diagrams have been observed which exhibit complete miscibility[27] or a closed-loop of immiscibility.[23,25,27] In the case of only two pairwise miscible polymers (A−B, A−C) in which the third pair (B−C) is immiscible, a sufficiently large concentration of A can occasionally produce a three-component miscible blend.[18−20,22] This is analogous to adding a good solvent to mix two immiscible polymers.

In the present study, two ternary blend systems have been studied, namely poly(styrene-*co*-methyl methacrylate), poly(methyl methacrylate), and polystyrene in which the copolymer has either a random or a strictly alternating sequence distribution. Styrene-centered homotriads (sss) comprise 10% and 0% of all the styrene-centered triads (sss, ssm, msm) of the random and alternating copolymers, respectively, as measured by NMR.[28] These copolymers permit the study of a controlled and small difference in sequence distribution. By synthesizing copolymers directly from distinct monomers, styrene and methyl methacrylate, our studies avoid the uncertainties caused by chemical ambiguities present in the chlorinated copolymers previously used for sequence distribution studies. The ternary blends of this study are in a previously little studied class in which none of the polymer pairs are miscible. Three-phase, three-component blends result and a direct imaging technique, namely transmission electron microscopy, is used to determine the number of phases, their relative amount, and their spatial arrangement. This information will be used to construct quantitative ternary phase diagrams, which are uncommon in experimental polymer science. The molecular weight dependence of the phase behavior in copolymer/PMMA blends, which exhibit partial miscibility, will also be explored. Finally, the implications of the observed asymmetry in miscibility will be discussed.

Experimental Methods

Polymers. Random copolymers of methyl methacrylate units and styrene units were synthesized via free-radical random copolymerization in a benzene solution with benzoyl peroxide as the initiator. Reactions were terminated at about 5% conversion by precipitating the polymer into methanol. The alternating copolymer was synthesized by complexing methyl methacrylate with ethylaluminum sesquichloride and the subsequent addition of styrene. The copolymers were fractionated using cold toluene−cyclohexane mixtures. Detailed polymerization procedures and characterization were reported previously.[9,14,28] Homopolymers of poly(methyl methacrylate) and polystyrene were purchased from Polymer Laboratories (Amherst, MA) or Polysciences, Inc. (Warrington, PA).

Table 1. Characteristics of Copolymers and Homopolymers

designation	M_w (g/mol) (SEC)[a]	M_w/M_n (SEC)[a]	mol % MMA (NMR)
Poly(styrene-*random*-methyl methacrylate)			
R72	72 000	1.60	47
R209	209 000	1.47	47
R286	286 000	1.49	48
Poly(styrene-*alternating*-methyl methacrylate)			
A279	279 000	1.41	50
A530	530 000	1.50	50
Poly(methyl methacrylate)			
M32	32 000	1.05	100
M108	108 000		100
Polystyrene			
S22	22 000	1.03	

[a] Copolymer and polystyrene molecular weight averages and polydispersities are reported as polystyrene equivalents; poly(methyl methacrylate) values are reported relative to poly(methyl methacrylate) standards.

Polymer Characterization. The molecular weights, polydispersities, and compositions of these polymers are reported in Table 1. Molecular weights and polydispersities were determined by size-exclusion chromatography using polystyrene and poly(methyl methacrylate) standards, as indicated. Copolymer composition and sequence distribution were determined from ^1H and ^{13}C solution NMR in hexachlorobutadiene. As previously reported,[9] random copolymers with ∼50 mol % MMA units have an alternating tendency, with only ∼10% of the triads occurring as homotriads. (A statistically random copolymer with 50 mol % composition would have 25% of the triads existing as homotriads.) The alternating copolymers are strictly alternating, that is having no homotriads and exactly 50 mol % MMA units. All copolymers and homopolymers are atactic.

Blend Preparation. Dilute solutions (∼1 w/v %) of copolymer and homopolymer(s) in anhydrous tetrahydrofuran (THF, Aldrich) were prepared in glass vials. THF is a good solvent for PMMA, PS, and their copolymers as suggested by the following solubility parameters given in $MPa^{1/2}$: THF, 18.6; PMMA, 17.4−27.2; PS, 16.06−20.2.[29] After the polymers dissolved, the solvent was evaporated at room temperature in an oven under an inert nitrogen gas flow for 2 days during which the blends formed films on the bottom and sides of the vial. The blends were gradually heated to 150 °C under a N_2 atmosphere and annealed at this temperature for 4−6 days. Anhydrous solvent and inert gas (N_2) were used during the solvent evaporation and annealing processes to minimize anomalous moisture effects known to occur in PMMA blends.[30] The blends were then quenched to room temperature and removed from the vials using a few drops of methanol and tweezers. Blends are identified as R 9/59/32, for example, in which the letter indicates whether the copolymer has a random (R) or an alternating (A) sequence and the numbers indicate the volume percent of the copolymer, poly(methyl methacrylate), and polystyrene, respectively. Unless indicated differently, the polymers contained in the blend are R286 or A279, M32, and S22, where the number represents the molecular weight in kg/mol. The following densities indicative of 150 °C were used to determine the volume fraction values: 1.19 g/cm^3 for poly(methyl methacrylate), 1.04 g/cm^3 for polystyrene, and 1.11 g/cm^3 for copolymers.[31] (The copolymer density was taken as a weighted average of the homopolymer densities.) The glass transitions of select blends were measured by differential scanning calorimetry using a Perkin-Elmer DSC7.

Electron Microscopy. Blend samples were stained, embedded, and microtomed prior to viewing them in an electron microscope. Small pieces (6 mm^2) of the film were placed on a glass slide under a crystallizing dish, along with an open

bottle of 0.5% aqueous ruthenium tetraoxide solution (Polysciences). The RuO_4 vapor selectively stained styrene monomeric units in the copolymer and homopolymer, so that immiscible phases with different styrene unit densities exhibit distinct gray levels in the microscope. Stained films were inserted into partially cured epoxy (Medacast Quik-Mix; Ted Pella, Redding, CA), after which the epoxy was allowed to fully cure overnight at 60 °C. The epoxy bullets were pretrimmed with a glass knife to expose part of the polymer film. Thin cross-sections (55−70 nm) of the embedded polymer were microtomed at room temperature using a 35° Diatome diamond knife and a Reichert Ultracut S. The sections floating on the water of the knife trough were transferred to 3 mm copper grids for transmission electron microscopy in a Philips 400T using a LaB_6 filament at 120 kV.

Image Analysis. When coexisting phases were apparently isotropically dispersed, the volume fraction of each phase was determined by applying the principle of stereology, which states that the volume fraction within a bulk sample equals the areal, line, or point fraction of a particular phase. This principle can readily be applied to TEM images if the projected distance, that is the thickness of the microtomed section ($\leq$0.07 μm), is much less than the domain size of the phase, typically $\geq$1 μm. Areal fraction measurements were obtained by digitizing negatives with a UC630 MaxColor scanner with a transmission attachment interfaced to a Macintosh IIci with Adobe Photoshop Image Editing software, the subsequent analysis using NIH Image 1.44 software.[32] The latter software measures the total area in an image and the area corresponding to a particular phase based on differences in the gray levels of the phases. Line fractions were measured by hand directly from the negatives by determining the fractional lengths of straight lines which correspond to a specific phase. Lines of a constant length were superimposed on the TEM negative in several random orientations to obtain an average measurement. For point fraction measurements, a grid of equally spaced points was superimposed on the negative, and the fraction of points lying on a particular phase was reported. Line or point fraction measurements were used when the contrast between the immiscible phases was low or the minority phase had a volume fraction less than approximately 15%. Multiple negatives (typically five) of each blend, which correspond to different areas of the same blend, were evaluated and the results averaged, yielding a typical standard deviation of 3 vol %.

Results

1. Blend Miscibility. The phase behavior of blends containing poly(styrene-*co*-methyl methacrylate) copolymer, polystyrene, and poly(methyl methacrylate) was determined using visual inspection, differential scanning calorimetry, and, most reliably, transmission electron microscopy. All three techniques agree in the case of blend R 92/8/0, which appears clear to the unaided eye and exhibits one glass transition at 105 °C. Given the glass transition temperatures of R286 and M32 are 104 and 120 °C, respectively, the measured T_g of this miscible blend is in agreement with the Fox equation. Figure 1 shows a transmission electron micrograph of this blend, showing a uniform gray level. (Subtle, parallel striations do appear on the micrograph and correspond to knife damage imposed during microtoming.) Thus, we conclude that R 92/8/0 is a one-phase blend and these three techniques of determining the phase behavior are in agreement.

However, this is not always the case as the two following examples will show. Blend R 67/33/0 is visually clear and exhibits two glass transition temperatures, 107 and 123 °C. These conflicting results were resolved using TEM to directly visualize the blend. Figure 2a shows that blend R 67/33/0 is a two-phase blend in which the majority phase stains more heavily, indicating a higher styrene repeat unit content. The minority phase forms domains which are comparable in size to the wavelengths of visible light; thus the blend appears transparent. Furthermore, the small difference

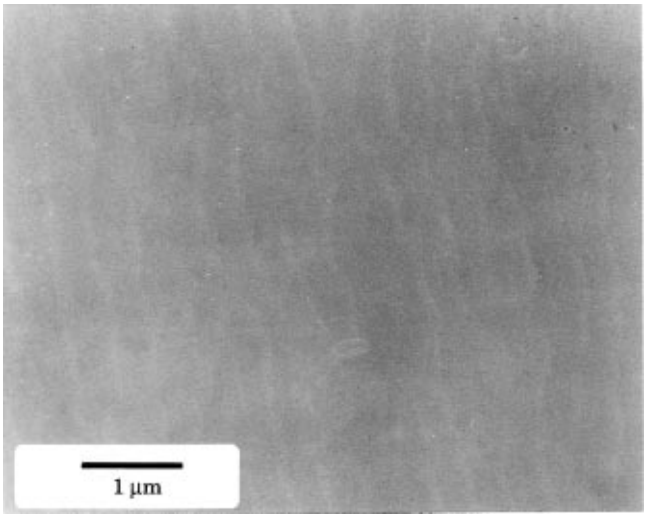

Figure 1. Transmission electron micrograph of R 92/8/0 exhibits a uniform gray level, indicating a miscible blend.

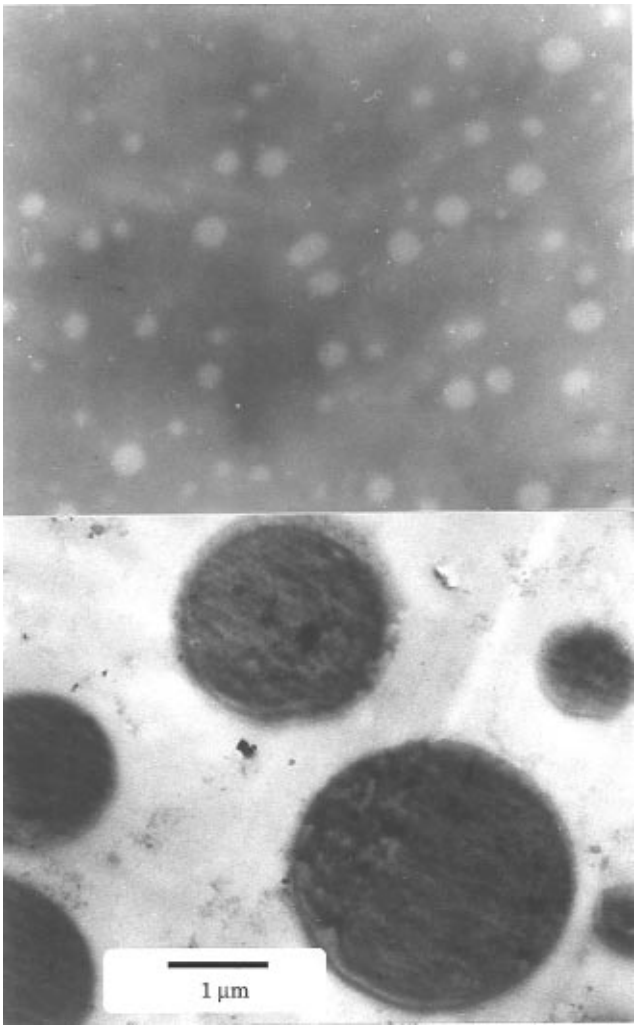

Figure 2. (a) Transmission electron micrograph of blend R 67/33/0 showing a second phase which is less stained, indicating that the minority phase contains less copolymer. (b) Blend A 33/32/35 exhibits two phases in which the isolated phase (dark) contains a larger fraction of styrene repeat units. Subsequently, the ternary phase diagram for this blend system indicated that the stained phase is predominantly homopolystyrene.

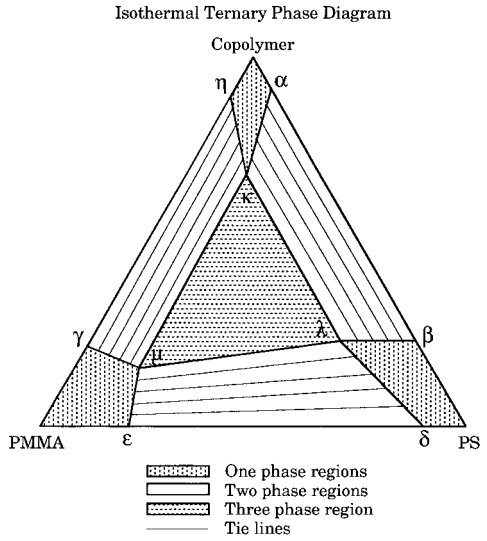

Figure 3. Schematic of a ternary phase diagram having three one-phase regions and one three-phase region. Blends on the sides of the ternary diagram have two components and the immiscible regimes fall between the following equilibrium compositions: copolymer and PS, α and β; PS and PMMA, δ and ϵ; PMMA and copolymer, γ and η. Ternary blends within the three-phase region phase separate into phases having equilibrium compositions of κ, λ, and μ. The tie lines within the two-phase regions are shown.

in the indices of refraction between the phases contributes to the misleading visual results.

In another example, blend A 33/32/35 appears cloudy, but exhibits only one glass transition at 99 °C. Electron microscopy of A 33/32/35, Figure 2b, clearly shows a two-phase blend in which the minority phase is heavily stained, indicating that the isolated domains contain more styrene repeat units, and also exhibits striations due to microtoming. Striations in the styrene-rich phase are frequently observed in our blends and arise due to the differences in mechanical properties between the phases. These striations provide an additional form of contrast between the phases in the TEM images. Blend A 33/32/35 contains approximately equal amounts of three components having glass transition temperatures in close proximity (i.e. 102 °C for A279, 120 °C for M32, and 99 °C for S22). In this blend, the glass transition temperatures of the two phases are indistinguishable in that only a single, broad glass transition was observed.

Transmission electron microscopy, or any direct imaging technique having suitable contrast and resolution, can resolve inconsistencies found between visual inspection and calorimetry. TEM can also provide unique information regarding the relative amounts of the different phases, which we have utilized to construct phase diagrams, as described in the next section. In addition, the arrangement of three coexisting phases such as encapsulation can be determined as discussed later in this paper.

2. Construction of Ternary Phase Diagrams. Quantitative phase diagrams provide two sets of information: compositions of equilibrium phases and relative amounts of these phases. Both pieces of information are important for understanding blend thermodynamics and for producing a blend with a particular set of properties. These statements apply equally well to both binary and ternary mixtures.

Figure 3 shows a schematic of an isothermal ternary phase diagram which has three one-phase regions and one three-phase region. (Temperature and pressure are fixed in this phase diagram, so that the two independent compositions can be plotted.) Every point within the equilateral triangle represents an overall ternary blend composition; points closer to an apex of the triangle correspond to compositions higher in the component indicated at that apex. Overall compositions which lie on the edges of the ternary phase diagram correspond to binary blends. For instance, blends represented by the line between the copolymer and PS apices are equivalent to blends along a horizontal, isothermal line in the copolymer−PS binary phase diagram plotted as temperature versus blend composition. Blends with compositions between the α and β phases will separate into two equilibrium phases of composition α and β, and the relative amounts of these phases are determined by the lever rule.

Ternary blends with overall compositions within a one-phase region are obviously miscible blends having equilibrium compositions equal to their overall compositions. If the overall composition of a ternary blend lies in a two-phase region, then the equilibrium compositions are given by the intersection of a tie line (shown as thin lines in Figure 3) with the phase boundaries, while the relative amounts of these phases are given by the lever rule. Ternary blends with overall compositions within the three-phase region phase separate into three equilibrium phases with compositions κ, λ, and μ. The relative amounts of these phases depend on the proximity of the overall blend composition to the apices of the triangular, three-phase region.

We have constructed ternary phase diagrams similar to that described above by knowing the overall blend composition, measuring the relative amounts of the equilibrium phases, and then calculating the equilibrium compositions using mass balances. An alternative approach to quantitative ternary phase diagrams would be to prepare many more blends, determine the number of phases present in each, and then draw the phase boundaries consistent with the data. While this approach might be acceptable for simple binary systems, extending this approach to ternary blends requires considerable material, which is particularly detrimental when working with model polymers as in this study. Using the principles of stereology, as described in the image analysis section above, the volume fraction of the various phases can be reliably determined from TEM images, if the images are representative of an isotropic sample. Two types of blends were evaluated. Two-component blends exhibiting two phases were used to determine the equilibrium compositions α, β, δ, ϵ, γ, and η; refer to Figure 3. Three-component blends exhibiting three phases were used to determine the equilibrium compositions κ, λ, and μ. Straight lines were drawn between these nine equilibrium compositions, which agree with the boundary rules[33] of phase diagrams; however, this procedure occasionally violates the boundary curvature rules.[34] These ternary phase diagrams represent a new level of quantification in experimental ternary polymer blends. The method which is further detailed below could be applied to any ternary system in which the relative amounts of the phases can be reliably measured.

Transmission electron micrographs of four blends containing R286 and M32 are shown in Figure 4. These blends each contain two components and phase separate into two phases. The darker phase contains a larger fraction of styrene repeat units and corresponds to the

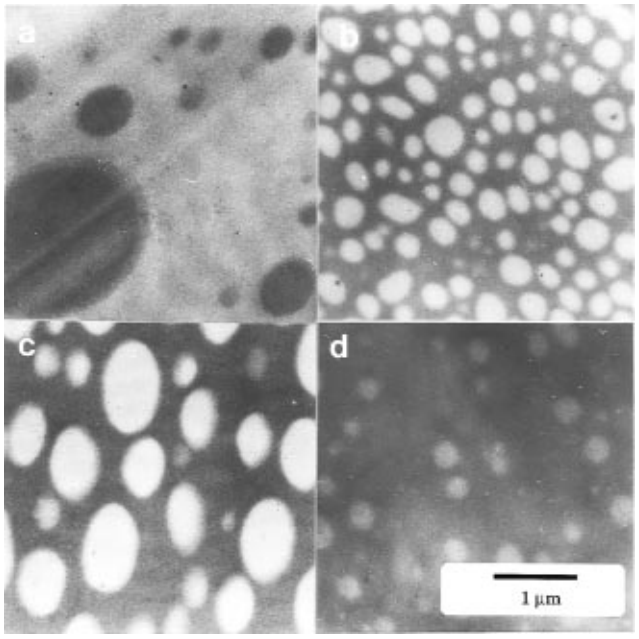

Figure 4. Transmission electron micrographs of four blends of increasing copolymer composition: (a) R 17/83/0, (b) R 48/52/0, (c) R 52/48/0, and (d) R 67/33/0. Note the phase inversion between (a) and (b) as the copolymer-rich phase (darker) changes from being the isolated phase to the continuous or matrix phase.

Table 2. Measured Area Fractions of R286/M32 Binary Blends Used To Calculate Equilibrium Compositions of the γ- and η-Phases

blends R286/M32/S22	no. of phases	area fraction of the copolymer-rich phase (η) in TEM images
16/83/0	2	0.18 ± 0.01
48/52/0	2	0.67 ± 0.02
52/48/0	2	0.62 ± 0.06
67/33/0	2	0.94 ± 0.01
92/8/0	1	
95/5/0	1	

copolymer-rich phase. As the copolymer composition increases from 16 vol % (Figure 4a) to 67 vol % (Figure 4d), the relative amount of the darker, copolymer-rich phase increases, as expected. Note, in particular, the phase inversion which occurs between 16 vol % (Figure 4a) and 48 vol % (Figure 4b), where the copolymer-rich phase changes from the isolated to the continuous phase of the blend. For each blend, the area fraction of the copolymer-rich phase is given in Table 2. As shown in Figure 3, phase-separated blends containing copolymer and PMMA have a PMMA-rich phase (γ) and a copolymer-rich phase (η), and the relative amount of the η-phase is given by the following lever rule:

$$V_\eta = \frac{\phi_{cop}^{blend} - \phi_{cop}^{\gamma}}{\phi_{cop}^{\eta} - \phi_{cop}^{\gamma}} \qquad (1)$$

where V_η is the volume fraction of the η-phase in the phase-separated blend, and ϕ_{cop}^{blend}, ϕ_{cop}^{γ}, and ϕ_{cop}^{η} are the volume fractions of copolymer in the blend, the γ-phase, and the η-phase, respectively. Linear regression is used to fit the experimental values of V_η and ϕ_{cop}^{blend} to determine $\phi_{cop}^{\gamma} = 0.06$ and $\phi_{cop}^{\eta} = 0.72$. Similar calculations were performed to determine the equilibrium compositions of the γ- and η-phases in the alterating copolymer case, as well as the α- and β-phases in both the random and the alternating copolymer cases. Binary blends of M32 and S22 phase separate, but image analysis of these blends to determine the volume fraction of the δ- or ϵ-phase was unreliable due to the large-scale phase separation, which prohibited the collection of representative images. Differential scanning calorimetry of these M32/S22 blends shows two distinct glass transitions which are similar to the transitions recorded for the individual components. Thus, the equilibrium compositions of the δ- and ϵ-phases were taken as pure S22 and pure M32, respectively.

Table 3. Comparison of the Measured and Calculated Volume Fractions of the κ-, λ-, and μ-Phases of the Random Copolymer Ternary Blends

blends R286/M32/S22	phase (i)	vol frac of phases (V_i) measd[a]	vol frac of phases (V_i) calcd[b]
9/66/24	κ	0.06 ± 0.01	0.10
	λ	0.22 ± 0.03	0.25
	μ	0.71 ± 0.04	0.66
32/34/34	κ	0.45 ± 0.02	0.44
	λ	0.35 ± 0.01	0.34
	μ	0.19 ± 0.02	0.22
46/43/11	κ	0.67 ± 0.01	0.64
	λ	0.11 ± 0.01	0.10
	μ	0.21 ± 0.02	0.26

[a] Image analysis of TEM data. [b] Mass balance calculations using the equilibrium compositions given in Figure 5 for the κ-, λ-, and μ-phases.

The relative amounts of the κ-, λ-, and μ-phases for R286/M32/S22 blends as measured by image analysis are given in Table 3. For example, blend R 9/66/24 exhibits 6 ± 1 vol % of the κ-phase, which contains the most copolymer and appears medium gray via TEM, 22 ± 3 vol % of the λ-phase, which contains primarily PS and appears dark gray with knife-induced striations, and 71 ± 4 vol % of the μ-phase, which contains primarily PMMA and appears light gray. (A TEM micrograph of this blend will be presented later, Figure 8a.) A mass balance for this system produces the following expressions of which only two equations are independent:

$$\phi_{cop}^{blend} = V_\kappa \phi_{cop}^{\kappa} + V_\lambda \phi_{cop}^{\lambda} + V_\mu \phi_{cop}^{\mu} \qquad (2)$$

$$\phi_{PS}^{blend} = V_\kappa \phi_{PS}^{\kappa} + V_\lambda \phi_{PS}^{\lambda} + V_\mu \phi_{PS}^{\mu} \qquad (3)$$

$$\phi_{PMMA}^{blend} = V_\kappa \phi_{PMMA}^{\kappa} + V_\lambda \phi_{PMMA}^{\lambda} + V_\mu \phi_{PMMA}^{\mu} \qquad (4)$$

where ϕ_i^j is the volume fraction of the i component (copolymer, PS, or PMMA) in the blend or j phase (κ, λ, or μ), the V_j is the volume fraction of the j phase in the blend. Using the known values of ϕ_i^{blend} and estimates of the ϕ_i^{κ}, ϕ_i^{λ}, and ϕ_i^{μ} values, values of V_κ, V_λ, and V_μ were calculated and compared to the measured values. The best agreement between measured and calculated volume fractions of the phases is shown in Table 3 and corresponds to the following equilibrium compositions in the R286/M32/S22 blend system: κ-phase, R 71/28/1; λ-phase, R 1/1/98, μ-phase, R 3/96/1. Table 4 shows the results for the alternating copolymer system, A279/M32/S22, in which the equilibrium compositions which best fit the measured volume fractions are κ-phase, A 40/54/6; λ-phase, A 9/20/71; and μ-phase, A 5/79/16. The calculated volume fraction is typically within the error of the measured volume fraction for a particular phase; the agreement is good.

Table 4. Comparison of the Measured and Calculated Volume Fractions of the κ-, λ-, and μ-Phases of the Alternating Copolymer Ternary Blends

blends A279/M32/S22	phase (i)	vol frac of phases (V_i) measd[a]	vol frac of phases (V_i) calcd[b]
14/62/24	κ	0.22 ± 0.05	0.24
	λ	0.23 ± 0.03	0.19
	μ	0.55 ± 0.08	0.58
25/56/20	κ	0.52 ± 0.03	0.55
	λ	0.19 ± 0.02	0.16
	μ	0.29 ± 0.02	0.29

[a] Image analysis of TEM data. [b] Mass balance calculations using the equilibrium compositions given in Figure 6 for the κ-, λ-, and μ-phases.

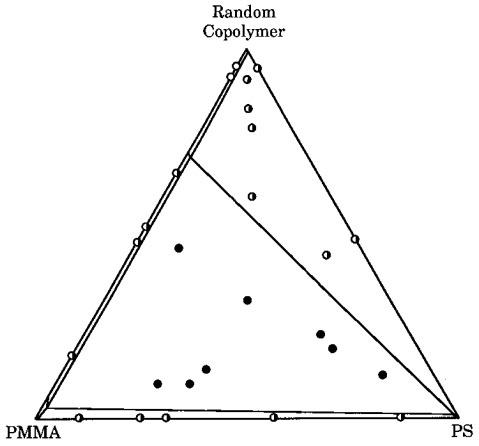

Phase Boundary Compositions
R286 / M32 / S22

α	100 / 0 / 0
β	0 / 0 / 100
δ	0 / 0 / 100
ε	0 / 100 / 0
γ	6 / 94 / 0
η	72 / 28 / 0
κ	71 / 28 / 1
λ	1 / 1 / 98
μ	3 / 96 / 1

Figure 5. Isothermal (T = 150 °C) ternary phase diagram for a random copolymer (R286), homopoly(methyl methacrylate) (M32), and homopolystyrene (S22). Open, half-filled, and filled circles indicate one-, two-, and three-phase behavior as determined by electron microscopy. The equilibrium compositions, as defined in Figure 3, were calculated as described in the text and are given here. Phase boundaries are drawn as straight lines between the equilibrium compositions.

The quantitative ternary phase diagrams are presented in Figures 5 and 6 for the random and alternating copolymers, respectively. Each circular symbol represents a blend which was examined using TEM. Open, half-filled, and filled circles correspond to one-, two-, and three-phase blends. Nine equilibrium compositions are listed below each diagram using the notation given in the schematic shown in Figure 3. The straight lines drawn between these equilibrium compositions in the ternary diagrams obey the boundary rules of ternary phase diagrams.[33] However, the boundary curvature rules are violated by the phase boundaries between the one- and two-phase regions near the PMMA apex in both the random and the alternating copolymer diagrams.[34] Curved phase boundaries could eliminate this violation, but there is insufficient information in the three-component, two-phase regions of the diagram to properly determine if the boundaries should be concave or convex.

3. Random Copolymer and Alternating Copolymer Ternary Phase Diagrams. The isothermal ternary phase diagrams shown in Figures 5 and 6 are for

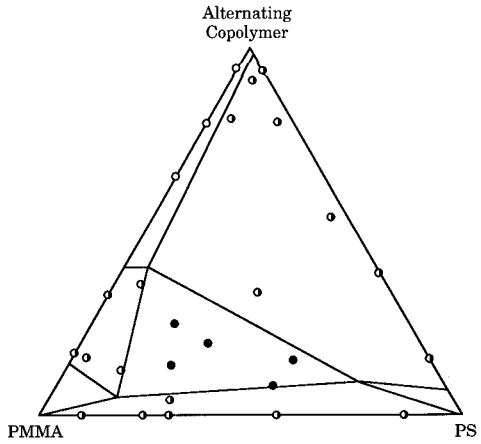

Phase Boundary Compositions
A279 / M32 / S22

α	98 / 0 / 2
β	7 / 0 / 93
δ	0 / 0 / 100
ε	0 / 100 / 0
γ	14 / 86 / 0
η	40 / 60 / 0
κ	40 / 54 / 6
λ	9 / 20 / 71
μ	5 / 79 / 16

Figure 6. Isothermal (T = 150 °C) ternary phase diagram for an alternating copolymer (A279), homopoly(methyl methacrylate) (M32), and homopolystyrene (S22). Refer to the previous figure caption for further details.

equivalent systems, with the exception of the sequence distibutions of the copolymers. The compositions, weight-averaged molecular weights, and the polydispersities of the copolymers are comparable, and the PMMA and PS are identical, leaving the sequence distribution of the copolymer as the sole variable between Figure 5 for the random copolymer and Figure 6 for the alternating copolymer. There are both similarities and differences in these ternary phase diagrams.

The isothermal ternary phase diagrams of both poly(styrene-*random*-methyl methacrylate) and poly(styrene-*alternating*-methyl methacrylate) with PMMA and PS exhibit one three-phase region, three two-phase regions, and three one-phase regions. This is the result of each of the corresponding binary and amorphous systems (copolymer/PS, copolymer/PMMA, PS/PMMA) being at least partially immiscible. Furthermore, our results indicate that the vast majority of the ternary blend compositions phase separate under near-equilibrium conditions at 150 °C into two or three coexisting phases. Namely, a copolymer, even a strictly alternating copolymer, is not sufficient to induce considerable between PMMA and PS at this temperature and these molecular weights.

Another characteristic feature of both ternary diagrams is the asymmetry of the one-phase region near the copolymer apex, which is the only sizable region of miscibility. Specifically, both copolymers are immiscible with PS over wide PS composition ranges: ~0−100% PS for the random sequence distribution and ~2−93% PS for the alternating sequence. However, the random copolymer is miscible up to ~28% PMMA and the alternating copolymer is miscible up to ~60% PMMA. Thus, both P(S-*co*-MMA) copolymers are more miscible with PMMA than with PS. A greater asymmetry is observed for the alternating copolymer, which subsequently produces a notably smaller three-phase region and larger two-phase regions, especially along the copolymer−PS edge.

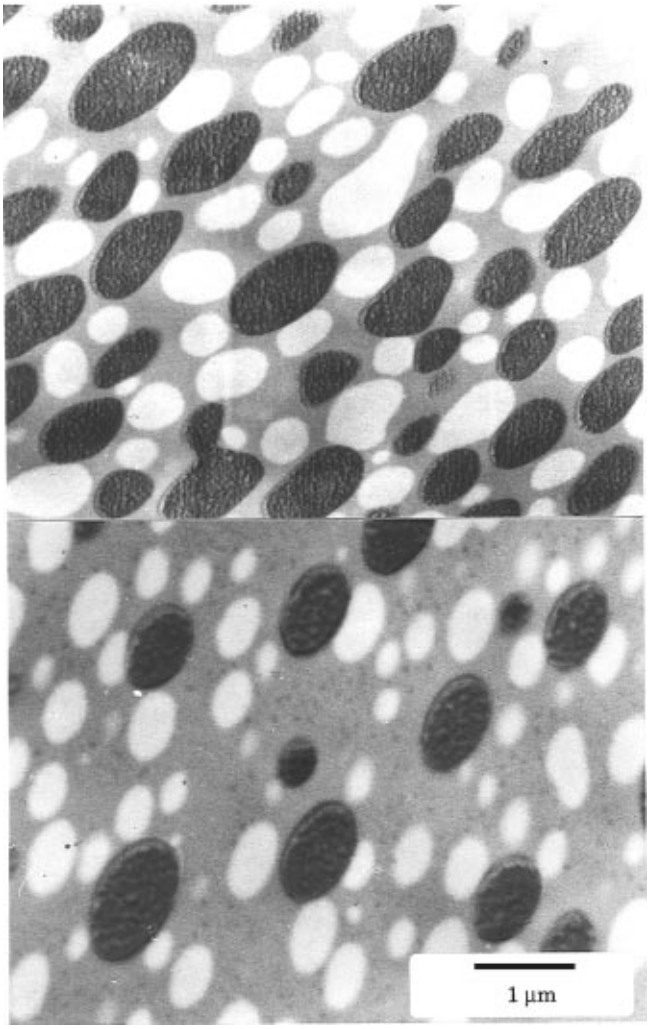

Figure 7. Transmission electron micrographs of three-phase blends in which the copolymer-rich phase (κ; medium gray) separates the PS-rich phase (λ; dark gray) and the PMMA-rich phase (μ; light gray) by forming a continuous matrix phase. (a) R 32/34/34; (b) R 46/43/11.

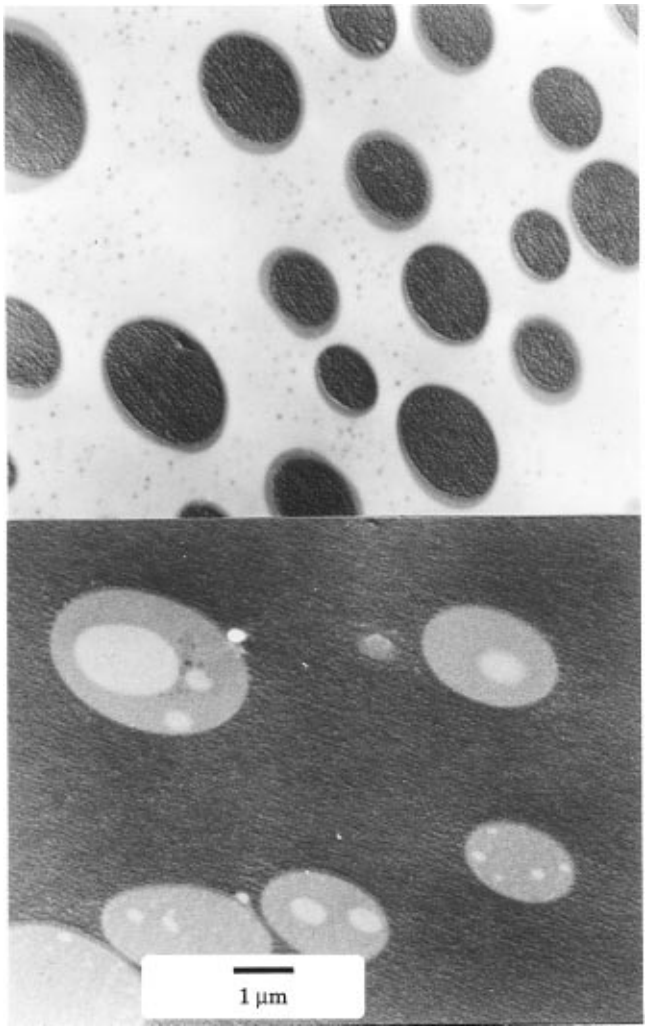

Figure 8. Transmission electron micrographs of three-phase blends in which the copolymer-rich phase (κ) separates the PS-rich phase (λ) and the PMMA-rich phase (μ) by encapsulating the minority component. (a) R 9/66/24, the κ-phase (medium) encapsulates the λ-phase (dark) within a continuous matrix of the μ-phase (light); (b) R 12/12/76, the κ-phase (medium) encapsulates the μ-phase (light) within a continuous matrix of the λ-phase (dark).

4. Morphology of Three-Phase Blends. As the phase diagrams indicate, both ternary systems exhibit three phases within a considerable portion of the overall blend compositions. Three-phase mixtures can be arranged either with or without encapsulation and both have been observed here. Figure 7 exhibits transmission electron micrographs of two blends, R 32/34/34 and R 46/43/11, in which the κ-phase (medium gray) forms a continuous matrix around the isolated domains of the λ-phase (dark) and μ-phase (light). Higher magnification images indicate that at least a small amount of the κ-phase separates the isolated domain of the λ- and μ-phases. Blend R 9/66/24 shows encapsulation, Figure 8a, in which the κ-phase encapsulates the minority λ-phase while the μ-phase forms a continuous matrix. Blend R 12/12/76 also shows encapsulation, but here the minority phase is the μ-phase, which is separated from the continuous λ-phase by the κ-phase. Similar results are found in blends containing alternating copolymer.

By examining all the three-phase blends in both blend systems, a number of generalizations can be made.

1. The κ-phase always separates the λ-phase from the μ-phase.

2. Encapsulation occurs when the κ-phase accounts for less than ~25 vol % of the blend, while the κ-phase forms a continuous matrix when it is more than ~32 vol % of the blend. In the blends having an intermediate amount of the κ-phase, both encapsulation and the absence of encapsulation were found in spatially separated regions of the blend sample.

3. These observations are common to both the random copolymer and alternating copolymer systems.

The first observation is consistent with the free energy driving force to reduce the interfacial energy of the system. The highest interfacial energy is expected between the λ-phase, the PS-rich phase, and the μ-phase, the PMMA-rich phase, while the interfacial energies between both the κ- and λ-phases and the κ- and μ-phases are expected to be lower due to a more similar chemical composition. Thus, the interfacial energy of the blend is minimized when the κ-phase separates the λ-phase from the μ-phase, as observed. In addition to these interfacial energies, the presence or absence of encapsulation depends on the relative amounts of the phases, and for these systems encapsulation is found in blends with <25 vol % of the κ-phase. However, because the presence or absence of encapsulation is sensitive to blend preparation, further investigation would be required to establish the encapsulation criteria for other processing methods. Finally, the interfacial

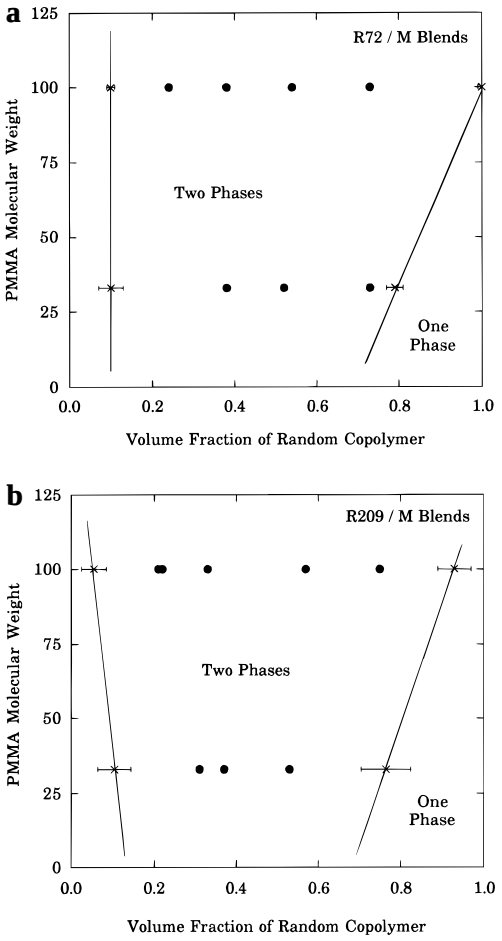

Figure 9. Phase boundaries as a function of homopolymer molecular weight in binary blends of random copolymer and homopoly(methyl methacrylate). (a) R72 and M; (b) R209 and M.

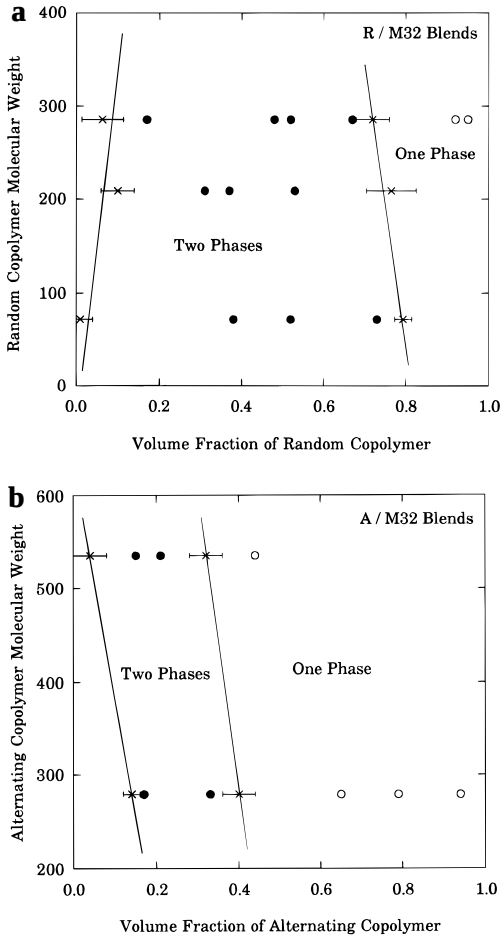

Figure 10. Phase boundaries as a function of copolymer molecular weight in binary blends of either a random copolymer (a) or an alternating copolymer (b) with homopoly(methyl methacrylate), M32.

energies of the random and alternating copolymers appear similar relative to the homopolymers, though a more sensitive probe of the interfacial energies may prove otherwise.

5. Molecular Weight Effect on Binary Phase Boundaries. Binary blends of random or alternating copolymer and PMMA were prepared to investigate the effect of molecular weight on the γ and η phase boundaries. As discussed in relation to the ternary phase diagrams, it is the partial miscibility of the P(S-*co*-MMA) copolymer and PMMA which profoundly influences the characteristics of the ternary phase diagram. Similar studies to show the effect of temperature were aborted, because preliminary DSC measurements indicated no measurable temperature dependence of the phase boundaries,[35] which is consistent with the weak temperature dependence of the PS−PMMA interaction parameter.[36]

The effect of the PMMA molecular weight is shown in Figure 9 in which the random copolymer molecular weight is held constant at either 72 000 or 209 000 g/mol. Miscible and immiscible blends are designated with open and filled circles, respectively, while the "x" corresponds to the γ and η phase boundaries, shown here with error bars. In both cases, increasing the PMMA homopolymer molecular weight from 32 000 to 108 000 g/mol significantly widens the immiscibility gap. As expected, raising the molecular weight of the lower molecular weight component significantly reduces miscibility. Figure 10 shows the effect of changing the copolymer molecular weight at a fixed PMMA molecular weight of 32 000 g/mol. Increasing the random copolymer molecular weight from 72 000 to 286 000 g/mol may slightly reduce with width of the immiscibility gap. Increasing the alternating copolymer molecular weight from 279 000 to 530 000 g/mol shifts the immiscibility gap to lower copolymer composition while maintaining a similar width. A comparison of Figures 10a and 10b further illustrates the sequence distribution effect in P(S-*co*-MMA) and PMMA blends; copolymers with the alternating sequence distribution exhibit greater miscibility with PMMA than the copolymers with the random sequence distribution.

Discussion

The copolymers studied here possess either a strictly alternating sequence of monomer units or a random sequence which has an alternating tendency. This relatively small difference in sequence distribution is sufficient to alter the isothermal ternary phase behavior in blends of poly(styrene-*co*-methyl methacrylate), poly(methyl methacrylate), and polystyrene, Figures 5 and 6. We find that the alternating copolymer exhibits greater miscibility with PMMA than the random copolymer, which implies that a smaller scale microstructure does improve miscibility. This trend is consistent with previous results from binary blends which compare sequence distributions other than random and strictly alternating: random and blocky poly(vinyl alcohol-*co*-vinyl acetate)[8] and chlorinated polyethylene and chlo-

rinated poly(vinyl chloride).[7] However, this improved miscibility was not observed between the copolymers and PS. Furthermore, neither sequence of P(S-*co*-MMA) copolymer is capable of inducing significant miscibility in the three-component blends. Alternatively, Piton and Natansohn have copolymerized both PS and PMMA with charge transfer agents to improve their miscibility, with some promising results.[37]

The ternary phase behavior in copolymer/homopolymer blends has been described using a Flory−Huggins and random phase approximation approach by Broseta and Fredrickson.[38] Their calculations are more appropriate for random copolymers than block copolymers, though the distinction between random and alternating sequences is not addressed. For the case of large incompatibilities and long copolymer chains, a broad three-phase region was predicted which consists of two homopolymer-rich phases and a copolymer-rich, or middle, phase. Also in this regime, the three binary systems were found to be immiscible. The condition of large incompatibilities was defined as $\chi N > 2(1 + [N/N_{AB}]^{1/2})^2$, where N is the homopolymer degree of polymerization (assumed to be equal for both A and B homopolymers) and N_{AB} is the copolymer degree of polymerization. Using published values for the temperature dependence of $\chi_{PS-PMMA}$[39] and the weight-averaged degrees of polymerization of our polymers, we determined that our isothermal ternary phase diagram meets their criteria of a highly incompatible ternary blend. The experimental ternary phase diagram for a random copolymer and two homopolymers which we report here is consistent with their predictions of a three-phase region and three immiscible binary pairs, though their calculations do not predict the asymmetry we observe in these ternary phase diagrams.

As indicated by our isothermal ternary phase diagrams, both PS−PMMA copolymers are more miscible with PMMA than with PS as illustrated by the asymmetric one-phase region near the copolymer apex of the ternary phase diagrams. That is, these compositionally symmetric AB-type copolymers are considerably more miscible with one homopolymer (A) than with the other homopolymer (B). Furthermore, this asymmetry in miscibility is greater for an alternating sequence distribution than a random sequence distribution. We speculate that the greater miscibility between the copolymers and PMMA is associated with weak attractive interactions between the MMA units of the copolymer and the homopolymer. These interactions are more effective in producing a miscible blend when the sequence distribution of the copolymer is strictly alternating. The random sequence distribution possesses short sequences with only styrene units which repel the PMMA molecule, while every styrene unit of a strictly alternating copolymer has a MMA unit on either side which can interact favorably with the PMMA homopolymer. Our hypothesis is supported by recent modeling work by Zhang et al. which indicates that the a specific interaction is capable of creating an asymmetric ternary phase diagram,[25] though the specific case of an AB copolymer blended with homopolymers A and B was not studied.

The asymmetry in the P(S-*co*-MMA)/PMMA/PS ternary phase diagrams has important implications when a random or alternating copolymer is confined to a PS/PMMA immiscible interface. At a sufficiently large copolymer coverage at a PMMA/PS interface a distinct layer of P(S-*co*-MMA) forms.[40] These miscibility results suggest that the copolymer/PMMA interface is broader and thus stronger than the copolymer/PS interface for compositionally symmetric copolymers. The mechanical properties of such copolymer layers are under investigation at present.[40]

The practical advantage of quantitative phase diagrams is their predictive capabilities with regard to the equilibrium compositions, relative amount of the phases, and, to a lesser extent, the arrangement of the phase. The scientific attraction to quantitative phase diagrams is the obvious ability to compare theory or simulations with experimental results. The methods employed here to construct phase diagrams represent a new level in experimental ternary polymer blends and could be applied widely. A direct imaging method is especially applicable when three or more phases are possible in a blend system, where the number of phases and relative amounts can be difficult to extract from nonimaging techniques. Furthermore, direct imaging explores encapsulation behavior in multicomponent blends, which could subsequently be used to produce a toughened plastic using a method analogous to two-stage emulsion particles having hard cores and rubbery shells. Simpler sample preparation and faster image analysis will continue to reduce the hours required to construct quantitative phase diagrams using this approach. Alternate experimental methods could be used to determine the relative amounts of the phases followed by a similar data analysis to construct quantitative ternary phase diagrams.

Acknowledgment. We acknowledge financial support from the Petroleum Research Foundation, administered by the American Chemical Society, the National Science Foundation (NSF-DMR-93-07993 and NSF-DMR-94-57997), and the Laboratory for Research on the Structure of Matter at the University of Pennsylvania (NSF-DMR-91-20668). A portion of these experiments were performed at AT&T Bell Laboratories while K.I.W. was a postdoctoral member of technical staff. Special thanks are given to Ms. Laura Cerini, who established the image analysis capabilities used here, Mr. Francis J. Gramkowski, who reanalyzed DSC data, and Ms. Nicole Pellegrini, who characterized the homopolymers.

References and Notes

(1) Allan, D. S.; Birchmeier, M.; Pribish, J. R.; Priddy, D. B.; Smith, P. B.; Hermans, C. *Macromolecules* **1993**, *26*, 6068.
(2) Masse, M. A.; Ueda, H.; Karasz, F. E. *Macromolecules* **1988**, *21*, 3438.
(3) Cowie, J. M. G.; Harris, J. H. *Polymer* **1992**, *33*, 4592.
(4) Ueda, H.; Karasz, F. E. *Polym. J.* **1992**, *24*, 1363.
(5) Zhikuan, C.; Ruona, S.; Karasz, F. E. *Macromolecules* **1992**, *25*, 6113.
(6) Dong, L.; Hill, D. J. T.; Whittaker, A. K.; Ghiggino, K. P. *Macromolecules* **1994**, *27*, 5912.
(7) Ueda, H.; Karasz, F. E. *Polym. J.* **1994**, *26*, 771.
(8) Isasi, J. R.; Cesteros, L. C.; Katime, I. *Polymer* **1995**, *36*, 1235.
(9) Galvin, M. E. *Macromolecules* **1991**, *24*, 6354.
(10) Balazs, A. C.; Karasz, F. E.; MacKnight, W. J.; Ueda, H.; Sanchez, I. C. *Macromolecules* **1985**, *18*, 2784.
(11) Balazs, A. C.; Sanchez, I. C.; Epstein, I. R.; Karasz, F. E.; MacKnight, W. J. *Macromolecules* **1985**, *18*, 2188.
(12) Balazs, A. C.; DeMeuse, M. T. *Macromolecules* **1989**, *22*, 4260.
(13) Cantow, H.-J.; Schulz, O. *Polym. Bull.* **1986**, *15*, 449.
(14) Galvin, M. E.; Heffner, S.; Winey, K. I. *Macromolecules* **1994**, *27*, 3520.
(15) Fredrickson, G. H.; Milner, S. T. *Phys. Rev. Lett.* **1991**, *67*, 835.
(16) Fredrickson, G. H.; Liu, A. J.; Bates, F. S. *Macromolecules* **1994**, *27*, 2503.
(17) Olmsted, P. D.; Milner, S. T. *Macromolecules* **1994**, *27*, 1964.

(18) Christiansen, W. H.; Paul, D. R.; Barlow, J. W. *J. Appl. Polym. Sci.* **1987**, *34*, 537.
(19) Ameduri, B.; Prud'homme, R. E. *Polymer* **1988**, *29*, 1052.
(20) Koklas, S. N.; Sotiropoulou, D. D.; Kallitsis, J. K.; Kalfoglou, N. K. *Polymer* **1991**, *32*, 66.
(21) Landry, C. J. T.; Yang, H.; Machell, J. S. *Polymer* **1991**, *32*, 44.
(22) Pomposo, J. A.; Calahorra, E.; Eguiazabal, I.; Cortazar, M. *Macromolecules* **1993**, *26*, 2104.
(23) Rabeony, M.; Siano, D. B.; Peiffer, D. G.; Siakali-Kioulafa, E.; Hadjichristidis, N. *Polymer* **1994**, *35*, 1033.
(24) Rigby, D.; Lin, J. L.; Roe, R. J. *Macromolecules* **1985**, *18*, 2269.
(25) Zhang, H.; Bhagwagar, D. E.; Graf, J. F.; Painter, P. C.; Coleman, M. M. *Polymer* **1994**, *35*, 5379.
(26) Min, K. E.; Chiou, J. S.; Barlow, J. W.; Paul, D. R. *Polymer* **1987**, *28*, 1721.
(27) Brannock, G. R.; Paul, D. R. *Macromolecules* **1990**, *23*, 5240.
(28) Heffner, S. A.; Bovey, F. A.; Verge, L. A.; Mirau, P. A.; Tonelli, A. E. *Macromolecules* **1986**, *19*, 1628.
(29) *Polymer Handbook*, 3rd ed.; Brandrup, J., Immergut, E. H., Eds.; John Wiley & Sons: New York, 1989.
(30) Cowie, J. M. G.; Miachon, S. *Macromolecules* **1992**, *25*, 3295.
(31) Kressler, J.; Higashida, N.; Shimomai, K.; Inoue, T.; Ougizawa, T. *Macromolecules* **1994**, *27*, 2448.
(32) Winey, K. I.; Galvin, M. E. In *51st Annual Meeting of the Microscopy Society of America*; San Francisco Press, Inc.: Cincinnati, OH, 1993; p 896.
(33) The boundary rule states that any region containing n phases can only be bounded by regions containing $n \pm 1$ phases. See: Gordon, P. *Principles of Phase Diagrams in Materials Systems*; Robert E. Krieger Publishing Co.: Malabar, FL, 1968; pp 186−188.
(34) The boundary curvature rule states that the boundaries of a one-phase region must meet with curvatures such that both boundaries extrapolate into either the adjacent two-phase regions or the adjacent three-phase region. See: Prince, A. *Alloy Phase Equilibria*; Elsevier Publishing Co.: New York, 1966; pp 143−145.
(35) Galvin, M. E., private communication, 1991.
(36) Russell, T. P. *Macromolecules* **1993**, *26*, 5819.
(37) Piton, M. C.; Natansohn, A. *Macromolecules* **1995**, *28*, 1605.
(38) Broseta, D.; Fredrickson, G. H. *J. Chem. Phys.* **1990**, *93*, 2927.
(39) Callaghan, T. A.; Paul, D. K. *Macromolecules* **1993**, *26*, 2439.
(40) Sikka, M.; Chen, W. L.; Pellegrini, N. N.; Winey, K. I., in preparation.

MA951434V